

Chebyshev Approximations of Feynman Integrals for Collider Physics

Samuel Abreu,^{a,b} Afonso Guerreiro,^{c,d} Ben Page^e

^a*CERN, Theoretical Physics Department, CH-1211 Geneva 23, Switzerland*

^b*Higgs Centre for Theoretical Physics, School of Physics and Astronomy, The University of Edinburgh, Edinburgh EH9 3FD, Scotland, United Kingdom*

^c*Instituto Superior Técnico (IST), Universidade de Lisboa, Av. Rovisco Pais 1, P-1049-001 Lisboa, Portugal*

^d*LIP, Av. Prof. Gama Pinto, 2, P-1649-003 Lisboa, Portugal*

^e*Department of Physics and Astronomy, Ghent University, 9000 Ghent, Belgium*

E-mail: samuel.abreu@cern.ch, afonsojg Guerreiro@tecnico.ulisboa.pt,
ben.page@ugent.be

ABSTRACT: We present a novel approach for solving canonical differential equations for Feynman integrals based on an approximation of the integrals with Chebyshev polynomials. By exploiting the analyticity properties of Feynman integrals, the method constructs rapidly converging polynomial approximations along a path, enabling highly efficient numerical evaluation. Moreover, we introduce an adaptive approximation method that dynamically samples to optimise convergence. We implement this framework in double-precision arithmetic and demonstrate its stability across physical phase space using a series of two-loop, five-point examples. Our proof-of-principle implementation proves competitive with state-of-the-art one-fold integral methods, while requiring little to no case-by-case intervention to handle spurious singularities.

Contents

1	Introduction	1
2	Canonical Differential Equations for Feynman Integrals	3
3	Chebyshev Approximations of Feynman Integrals	4
3.1	Chebyshev Series and Interpolants	5
3.2	Working with Chebyshev Series	9
3.3	Numerical Convergence of Chebyshev Series	13
3.4	An Adaptive Chebyshev Approach for Feynman Integrals	16
4	Application to Pentagon Functions	19
4.1	Physical Phase Space for Five-Point Processes	19
4.2	Numerical Study for Five-Point Massless and One-Mass Scattering	21
4.3	Ancillary Files	24
5	Summary and Outlook	25

1 Introduction

Feynman integrals are fundamental building blocks required to carry out computations in Quantum Field Theory. Their evaluation is essential for precisely probing the Standard Model and searching for new physics. In the context of high-energy collision experiments [1–3], the increase in experimental precision demands the inclusion of higher-order terms in perturbation theory, thereby necessitating the calculation of multi-loop Feynman integrals. The systematic evaluation of such integrals, particularly in the presence of multiple kinematic scales, remains an active area of research. Currently, the state-of-the-art approach consists of reducing all Feynman integrals arising in a given calculation to a smaller set of master integrals via systematic use of integration-by-parts (IBP) identities [4]. The solution of the IBP identities is obtained with Laporta’s algorithm [5], which has been implemented in many public codes [6–11].

While there exist many techniques for the evaluation of master integrals (see, e.g. [12, 13] for detailed reviews), the most prominent among them is the method of differential equations [14–18]. Here, one differentiates the master integrals with respect to kinematical variables and internal masses, leading to a system of first-order differential equations whose solution yields the master integrals. In many cases, this system can be cast into so-called “canonical form” [19] in which the dependence on the dimensional regulator, ϵ , factorises, and the integration kernels are $d \log$ forms. In this form, the differential equations admit a straightforward solution in terms of iterated integrals, which can often be expressed in

terms of multiple polylogarithms. Furthermore, for multi-scale problems, even when such a basis can be found, finding an analytic solution is often prohibitively difficult and one must often reach for numerical methods.

To address this issue, several numerical methods have been developed for solving the differential equations satisfied by the master integrals. One such method relies on power-series expansions to construct local solutions [20, 21]. This technique has been implemented in the publicly available `Mathematica` packages `DIFFEXP` [22] and `SEASIDE` [23]. A similar idea underpins the auxiliary mass flow method [24, 25], which has also been implemented in the `Mathematica` package `AMFLOW` [26]. These implementations are widely used to provide boundary conditions and evolve a solution over phase-space. However, despite this success, they often exhibit long runtimes, making them challenging to adopt for phenomenological applications. The package `LINE` [27] seeks to mitigate these performance limitations by adopting a C++ implementation of the auxiliary mass flow method. Moreover, recent investigations into novel techniques for numerically solving differential equations such as Runge-Kutta and Bulirsch-Stoer integration [28–31] have shown impressive runtime for frontier two-loop examples, and analogous approaches are being explored to numerically compute iterated integrals [32]. More recently, pseudo-spectral methods have been proposed and demonstrated for the evaluation of two-loop massless six-point integrals [33], resulting in highly accurate numerical evaluations.

In this work, we propose an alternative approach based on global expansions in terms of Chebyshev polynomials to approximate a given target function. This sets the method apart from local expansion schemes, such as those based upon generalised power series expansions. Since first being introduced in the context of numerical fluid dynamics (see [34, 35]), they have been applied in numerous contexts spanning from meteorology and climate modelling [36] to numerical general relativity [37]. Their increasing popularity can be largely attributed to their excellent convergence properties: for analytic functions, their convergence is exponential. This feature motivates our study of their use in applications to Feynman integrals, whose region of analyticity is becoming increasingly well understood in recent years [38–44].

In this work, we exploit the suitability of Chebyshev polynomials to approximate analytic functions in order to construct an efficient method for numerically evaluating multi-scale Feynman integrals over physical phase space. Our approach leverages modern understanding of numerical construction of Chebyshev approximations. Specifically, we use tools introduced in the `chebfun` project [45–47] to construct an adaptive Chebyshev approximation method that avoids oversampling in the presence of roundoff error and nearby non-analyticities, optimizing convergence. We study our approach in applications to two-loop five-point Feynman integrals, stress testing our algorithm by using it to evaluate so-called “pentagon functions” for full-colour five-point massless matrix elements and leading-colour five-point one-mass matrix elements. In practice, we find that the approach is numerically stable, and is insensitive to the presence of spurious singularities of the differential equation. Comparing it to cutting-edge implementations of one-fold integration techniques [48, 49], we find competitive runtimes and stability properties. We provide a proof of principle `Mathematica` implementation in ancillary files to enable future study.

This work is structured as follows. In section 2, we introduce the necessary details of canonical differential equations for Feynman integrals. In section 3, we describe our Chebyshev-based solution method. We begin by discussing the basic theory of Chebyshev polynomials and Chebyshev interpolants as well as their convergence properties in numerical applications. We then discuss our adaptive Chebyshev approximation approach. In section 4, we apply our approach to a collection of two-loop five-point Feynman integrals, and study their numerical stability over phase space, providing a proof-of-concept approach in ancillary files.

2 Canonical Differential Equations for Feynman Integrals

In this work, we are interested in studying the application of Chebyshev polynomial approximation methods to solve the differential equations that Feynman integrals satisfy [14–19]. In recent years, the differential equations method has become one of the most commonly used approaches for computing Feynman integrals—prominently in the case of multi-scale Feynman integrals. Denoting a basis of master integrals as \vec{J} , the integrals are functions of the kinematic invariants \vec{s} and the dimensional regulator $\epsilon = (4 - D)/2$. Such a basis of master integrals satisfies a first-order partial differential equation as

$$dJ_i = A_{ij}(\vec{s}, \epsilon)J_j, \quad (2.1)$$

where the $A(\vec{s}, \epsilon)$ are matrices of one forms that are rational in the invariants \vec{s} and ϵ . If one has such a system of differential equations to hand, the problem of computing the collection of Feynman integrals is reduced to evaluating an appropriate boundary condition and solving the differential equation to evolve this boundary condition to another point in the physical phase space.

The difficulty of solving the differential equation can be alleviated by an appropriate choice of basis. If we consider the differential equation for a different basis of Feynman integrals \vec{I} related to \vec{J} via $J_i = U_{ij}I_j$, then the new basis satisfies the differential equation

$$dI_i = \tilde{A}_{ij}I_j, \quad \text{where} \quad \tilde{A} = U^{-1}AU - U^{-1}dU. \quad (2.2)$$

In practice, solving the differential equation is arguably the simplest if one works with a basis of master integrals that satisfies a differential equation that is in so-called “canonical form” [19]. If \vec{I} is such a basis, then eq. (2.2) simplifies to the form

$$dI_i = \epsilon M_{ijk} d \log(W_j) I_k, \quad (2.3)$$

where $\epsilon = (4 - D)/2$ is the dimensional regulator, the coefficients M_{ijk} are rational numbers, and the arguments W_j are algebraic functions of the kinematics. The analytic structure of these Feynman integrals is strictly controlled by the collection of W_j , which are typically referred to as the “letters” of the alphabet. Not all collections of Feynman integrals admit a basis that satisfies a canonical differential equation as defined above, for example in the presence of elliptic integrals. While it would be interesting to study the application of our approach to such Feynman integrals, we leave this to future work.

For phenomenological applications of Feynman integrals in collider physics, the principal aim is to evaluate the integrals as a series expansion in ϵ . This task is greatly facilitated by the ϵ -factorised form of the canonical differential equation in eq. (2.3) as one can write the series expansion of the vector of integrals as

$$I_i(\vec{s}, \epsilon) = \sum_{n=0}^{\infty} \epsilon^n I_i^{(n)}(\vec{s}), \quad (2.4)$$

where the ϵ expansion order n denotes the weight of the integral. By inserting eq. (2.4) into eq. (2.3), one concludes that the coefficients of the ϵ expansion satisfy an iterative tower of differential equations given by

$$dI_i^{(n)} = M_{ijk} d \log(W_j) I_k^{(n-1)}. \quad (2.5)$$

Importantly, while the integrals I_i are linearly independent to all orders in ϵ , the individual coefficients $I_i^{(n)}$ can exhibit linear dependencies. It is therefore natural to consider solving for an independent set of functions that span the space at each weight, which we will denote as $\tilde{I}_i^{(n)}$. In ref. [50], it was proposed that linear dependencies between functions can be easily resolved by working at the symbol level, supplemented by a small number of constraints from numerical evaluations. This procedure generates both the basis $\tilde{I}_i^{(n)}$ and a rational number matrix $A_{ij}^{(n)}$ such that the original coefficients map to the basis via $I_i^{(n)} = A_{ij}^{(n)} \tilde{I}_j^{(n)}$. Using this information, it is systematic to construct a differential equation for the independent special functions of the form

$$d\tilde{I}_i^{(n)} = \tilde{M}_{ijk}^{(n)} d \log(W_j) \tilde{I}_k^{(n-1)}, \quad (2.6)$$

where the $\tilde{M}_{ijk}^{(n)}$ are rational numbers and $n \geq 1$.

The differential equation in eq. (2.6) is particularly appealing as its formal solution along a path can easily be achieved by direct integration. Let us consider a path in Mandelstam space $\vec{s}(t)$, which starts at $t = 0$ and ends at $t = 1$. If we assume the availability of a boundary value $I^{(n)}(\vec{s}_0)$, one can then directly write

$$\tilde{I}_i^{(n)}(\vec{s}[t]) = \tilde{I}_i^{(n)}(\vec{s}_0) + \int_0^t dt' M_{ijk}^{(n)} \frac{\partial}{\partial t'} \log(W_j[\vec{s}(t')]) \tilde{I}_k^{(n-1)}(\vec{s}[t']). \quad (2.7)$$

The challenge in applying eq. (2.7) is to perform the integration on the right-hand side. If performed analytically, this integration leads to the introduction of dedicated classes of special functions such as generalised polylogarithms. Alternatively, if one can find an analytic representation for the integrands in eq. (2.7), one can compute these integrals numerically, as done in [48–50]. In this work, we take yet another alternative, quasi-numerical, route. We will explore computing the integrals in eq. (2.7) by using the differential equations to approximate the $\tilde{I}_i^{(n)}(\vec{s}[t])$ using Chebyshev polynomials.

3 Chebyshev Approximations of Feynman Integrals

In recent years, a popular method that has arisen for solving the differential equations that Feynman integrals satisfy, eq. (2.1), is that of “generalised power series expansion” [20–23, 26, 27]. Here, one begins by choosing a univariate path $\vec{s}(t)$ in phase space between

an initial point \vec{s}_0 and a final point \vec{s}_1 where the value of the set of Feynman integrals is desired. The Feynman integrals are then locally represented as generalised power series in the path parameter t , constrained to satisfy the differential equation. This allows both for a systematic evaluation of the set of Feynman integrals at the point \vec{s}_1 , as well as a quasi-analytic solution for the Feynman integral everywhere along the path.

One of the practical difficulties of this approach is that singularities of the differential equation which live in the complex t -plane can limit the radius of convergence of a generalised power series centred at \vec{s}_0 so that it does not include the point \vec{s}_1 . The common solution to this problem is to employ a collection of power-series solutions, each with an overlapping region of convergence, which continuously cover the integration path and thereby evolve the solution from \vec{s}_0 to \vec{s}_1 . Nevertheless, from both a practical and physical perspective, this feature is undesirable. Specifically, when evolving over paths contained within physical phase-space, singularities that lie directly along the path are very rarely encountered (see e.g. ref. [50] for an example arising in non-planar Feynman integrals). Moreover, in recent years, our understanding of the location of singularities of Feynman integrals has become increasingly systematic [38–44]. It is therefore natural to ask if there exists a method that is similarly powerful to power series expansion, but is (in principle) only sensitive to singularities that lie along the integration path, not in the complex t -plane. In this section, we discuss how a representation of Feynman integrals as a ‘‘Chebyshev series’’ can answer this question. We will begin by introducing the necessary theoretical background on Chebyshev series, then discuss how they can be manipulated, and finally discuss how they can be constructed in a practical manner that ensures numerical stability.

3.1 Chebyshev Series and Interpolants

The starting point for our discussion is the following important result [51]: any sufficiently continuous¹ function $f(x)$ defined on the interval $[-1, 1]$ admits a unique representation as a ‘‘Chebyshev series’’. Specifically, one can write:

$$f(x) = \sum_{k=0}^{\infty} a_k T_k(x), \quad a_k = \frac{2}{(1 + \delta_{k0})\pi} \int_{-1}^1 \frac{f(x) T_k(x)}{\sqrt{1-x^2}} dx, \quad (3.1)$$

where the $T_k(x)$ are polynomials of degree k in x known as the ‘‘Chebyshev polynomials of the first kind’’. For ease we will refer to the $T_k(x)$ simply as Chebyshev polynomials. Such Chebyshev polynomials can be defined implicitly through the relation

$$T_k(\cos \theta) = \cos k\theta, \quad (3.2)$$

where standard trigonometric relations make it clear that the right hand side is a polynomial in $\cos(\theta)$. A comprehensive discussion of Chebyshev polynomials can be found in ref. [52]. Note that, even though eq. (3.1) applies to the interval $[-1, 1]$, we may extend its

¹The details of the continuity assumption here are somewhat technical. Lipschitz continuity is sufficient for absolute convergence, while for pointwise convergence continuity is sufficient. Furthermore, for uniform convergence, a sufficient condition is that the function should have bounded variation or satisfy the Dini-Lipschitz condition [52].

application to any finite interval $[a, b]$ via some function that maps $[a, b] \leftrightarrow [-1, 1]$. (We will return to the question of choosing a suitable map in section 3.4.)

To consider the convergence properties of Chebyshev series in more detail, let us introduce the concept of a ‘‘Bernstein ellipse’’ [53, 54]. This is defined as the image of a complex circle $|z| = \rho$ which is centred at the origin, under the ‘‘Joukowski map’’

$$z \mapsto \frac{z + z^{-1}}{2}. \quad (3.3)$$

For $\rho > 1$, this mapping yields an ellipse in the complex plane with foci at $z = \pm 1$. Its major (minor) semi-axis a (b) is given in terms of ρ by

$$a = \frac{1}{2}(\rho + \rho^{-1}), \quad b = \frac{1}{2}(\rho - \rho^{-1}). \quad (3.4)$$

Now, let E_ρ denote the interior of the largest Bernstein ellipse to which f can be extended analytically. For our purposes, the importance of this Bernstein ellipse is that the Chebyshev series of f converges inside E_ρ and diverges everywhere outside it [55].

The parameter ρ is determined by the location of the nearest singularity of f to the interval $[-1, 1]$ in the complex plane, i.e. the closest point beyond which f can no longer be analytically continued. If the convergence-limiting singularity is located at $z_0 = x_0 + iy_0$ in the complex plane, then the parameter ρ for the largest admissible Bernstein ellipse is given by:

$$\rho = \alpha + \sqrt{\alpha^2 - 1}, \quad \alpha = \frac{1}{2} \left[\sqrt{(x_0 + 1)^2 + y_0^2} + \sqrt{(x_0 - 1)^2 + y_0^2} \right] \quad (3.5)$$

Note that the interval $[-1, 1]$ is always contained within E_ρ . As such, any singularity of $f(x)$ that lies outside $[-1, 1]$ may slow the convergence of the series, but it can never spoil it. For our applications to Feynman integrals, the importance of this statement is that if a Feynman integral is sufficiently continuous along a path, then it can be represented by a single Chebyshev series.

For clarity, let us illustrate this discussion with a physical example. Specifically, we consider the pure equal mass one-loop bubble in 2 dimensions,

$$I_{\text{bub}}(s, m^2) = \log \left(\frac{\sqrt{4m^2 - s} - i\sqrt{s}}{\sqrt{4m^2 - s} + i\sqrt{s}} \right), \quad (3.6)$$

which has branch points at $s = 4m^2$ and $s = 0$ with branch cuts for $s \in [4m^2, \infty)$ and $s \in (-\infty, 0]$. Naturally, $I_{\text{bub}}(s, m^2 = 1)$ is not analytic for $s \in [-1, 1]$. However, we can easily map $x \in [-1, 1]$ to some other interval $[a, b]$ through

$$s(x) = b - (b - a) \frac{1 - x}{2}. \quad (3.7)$$

For concreteness, we choose the interval $[1/2, 3]$, where $I_{\text{bub}}(s, m^2 = 1)$ is analytic. The region of convergence of the Chebyshev series is determined by the largest (mapped) Bernstein ellipse whose interior contains no singularities of $I_{\text{bub}}(s, 1)$. The closest branch point

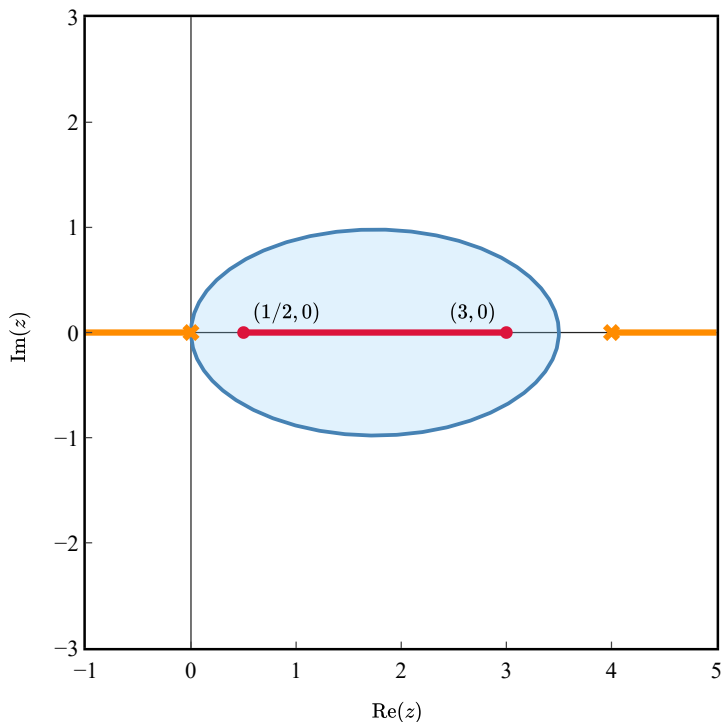


Figure 1: Region of convergence for the Chebyshev series representation of the pure 2-dimensional massive bubble integral $I_{\text{bub}}(s, m^2 = 1)$. The crimson dots at $(1/2, 0)$ and $(3, 0)$ indicate the foci of the ellipse, while the orange crosses (lines) represent the branch points (cuts) of $I(s, 1)$.

to the interval $[1/2, 3]$ is located at $s = 0$; therefore, the parameter corresponding to the largest admissible Bernstein ellipse is $\rho \approx 2.380$. The region of convergence of the Chebyshev interpolation of $I_{\text{bub}}(s, m^2 = 1)$ is illustrated in fig. 1.

Naturally, in computational applications, one cannot work directly with the infinite expansion in eq. (3.1). Rather, we must construct a finite sum of Chebyshev polynomials. One approach to do this would be to truncate the series, keeping only the first $n + 1$ terms. However, the difficulty of computing the coefficients a_k via the weighted integral in eq. (3.1) means that this approach is rarely used in practice. Alternatively, we can use interpolation. Specifically, we will construct a Chebyshev series that agrees with the function f at a finite set of $n + 1$ so-called Chebyshev nodes.² We will work with the so-called “Chebyshev nodes of the second kind” or “Chebyshev-Lobatto nodes”. These are defined to be the

²Importantly, Chebyshev grids often outperform alternative node distributions such as equidistant grids. A textbook example is provided by Runge’s phenomenon, in which polynomial interpolation on equidistant nodes exhibits increasingly large oscillations near the endpoints of the interval $[-1, 1]$, leading to a catastrophic loss of accuracy. By contrast, interpolation on Chebyshev nodes is immune to this instability, converging uniformly on $[-1, 1]$.

$n + 1$ extrema of the n -th Chebyshev polynomial, and are located at

$$x_j = \cos\left(\frac{j}{n}\pi\right), \quad j \in \{0, \dots, n\}. \quad (3.8)$$

We define a Chebyshev interpolant of $f(x)$ of order n to be the unique polynomial p_n of degree n which matches $f(x)$ on $n + 1$ Chebyshev-Lobatto nodes. That is,

$$p_n(x_k) = f(x_k). \quad (3.9)$$

While such a polynomial can be represented using standard interpolation techniques in terms of so-called Lagrange cardinal polynomials [51], it is more natural to express it in terms of the Chebyshev basis as

$$p_n(x) = \sum_{k=0}^n \hat{a}_k T_k(x). \quad (3.10)$$

Importantly, the coefficients of this Chebyshev expansion, \hat{a}_k , can be computed efficiently as we will discuss in section 3.2. We note that interpolation generally yields a different polynomial approximation from that obtained via truncation. That is, for a given $f(x)$, $a_k \neq \hat{a}_k$ in eqs (3.1) and (3.10). Nevertheless, both constructions share similar convergence properties while typically yielding approximations of comparable accuracy and we thus choose to focus on interpolation for the remainder of this work.

In practice, the convergence of a Chebyshev interpolant is intimately related to the smoothness of the function being approximated. As a general rule of thumb, the smoother the function, the faster the rate of convergence. This observation can be made precise through the following theorems (for further details, we refer the reader to ref. [51]), beginning with a result concerning differentiable functions. Let $m \in \mathbb{N}_0$, and suppose that $f(x)$ and its derivatives up to $f^{(m-1)}$ are absolutely continuous on $[-1, 1]$, while the m -th derivative has finite variation³ V . Under these conditions, it can be shown that the coefficients of the Chebyshev interpolant of $f(x)$ satisfy

$$|\hat{a}_k| \leq \frac{2V}{\pi(k-m)^{m+1}}, \quad (3.11)$$

for all $k > m$. Moreover, there is a well-behaved bound on the interpolation error associated to $p_n(x)$. Using this, under the previous conditions, it can be shown that $p_n(x)$ satisfies

$$\|f(x) - p_n(x)\|_\infty \leq \frac{4V}{\pi m(n-m)^m}, \quad n > m, \quad (3.12)$$

where $\|g(x)\|_\infty$ is the sup-norm of $g(x)$ on the range $[-1, 1]$, i.e.

$$\|g(x)\|_\infty = \sup\{|g(x)| : x \in [-1, 1]\}. \quad (3.13)$$

That is, the largest error across the interpolation range falls algebraically with increasing n .

³Letting f be differentiable with a Riemann-integrable first derivative, one defines the ‘‘variation of f ’’ on an interval $[a, b]$ as $V = \int_a^b |f'(x)| dx$.

The algebraic rate of convergence for differentiable functions is greatly improved when one considers analytic functions instead. In this case, the relevant result states that if $f(x)$ is analytic on $[-1, 1]$ and admits an analytic continuation to the open Bernstein ellipse E_ρ , and if $|f(z)| < M$ for some $M > 0$ and all $z \in E_\rho$, then its Chebyshev coefficients satisfy

$$|\hat{a}_0| \leq M, \quad |\hat{a}_k| \leq 2M\rho^{-k}, \quad (3.14)$$

for all $k \geq 1$, while the interpolation error in the sup-norm satisfies

$$\|f(x) - p_n(x)\|_\infty \leq \frac{4M\rho^{-n}}{\rho - 1} \quad (3.15)$$

for all $n \geq 0$. That is, Chebyshev interpolation achieves geometric convergence for analytic functions across the interpolation range⁴. Eq. (3.15) is the main motivation for exploring the use of Chebyshev polynomials to approximate Feynman integrals: if we restrict to a segment of phase-space inside of the well understood regions of analyticity, then we find that we can obtain a useful approximation with comparatively low approximation order.

To illustrate the convergence properties of Chebyshev interpolants, let us return to the example of the bubble integral in eq. (3.6). We interpolate $I_{\text{bub}}(s, m^2 = 1)$ over two intervals $s \in [-1, 1]$ and $s \in [1/2, 3]$ as shown in fig. 2. Since $I_{\text{bub}}(s, 1)$ is analytic in a neighbourhood of $[1/2, 3]$, the corresponding Chebyshev expansions exhibit geometric convergence. This is reflected in the asymptotically linear decay of the expansion coefficients on a logarithmic scale. In contrast, $I_{\text{bub}}(s, 1)$ is continuous but not differentiable at $s = 0$. Hence, the interpolant on $[-1, 1]$ exhibits only algebraic convergence. This is evidenced by a departure from linear behaviour, with coefficients bending upward, away from a straight line, with a slope that tends to zero from below.

3.2 Working with Chebyshev Series

Having motivated that Chebyshev series constructed via interpolation provide a valuable method of approximation for Feynman integrals, let us now discuss the necessary tools for working with them to achieve our goals of approximating the integrals in eq. (2.7). In practice, this set is quite limited which adds to the attractiveness of the approach. We must know how to construct a Chebyshev series via interpolation, compute the anti-derivative and evaluate a Chebyshev series to match the boundary condition in eq. (2.7).

Constructing a Chebyshev Interpolant Let us consider the problem of computing an order n Chebyshev interpolant $p_n(x)$ for a given function $f(x)$. That is, we wish to construct the set of coefficients \hat{a}_k of eq. (3.10). Mathematically, this can be achieved by leveraging the discrete orthogonality condition satisfied by the Chebyshev polynomials [52],

$$\sum_{k=0}^n {}''T_i(x_k)T_j(x_k) = \begin{cases} 0, & i \neq j \quad \text{and} \quad i, j \leq n \\ \frac{n}{2}, & i = j \quad \text{and} \quad 0 < i < n \\ n, & i = j \quad \text{and either} \quad i = 0 \quad \text{or} \quad i = n, \end{cases} \quad (3.16)$$

⁴For entire functions, one finds super-geometric convergence since the Bernstein parameter ρ can be taken arbitrarily large, leading to decay faster than any fixed geometric sequence.

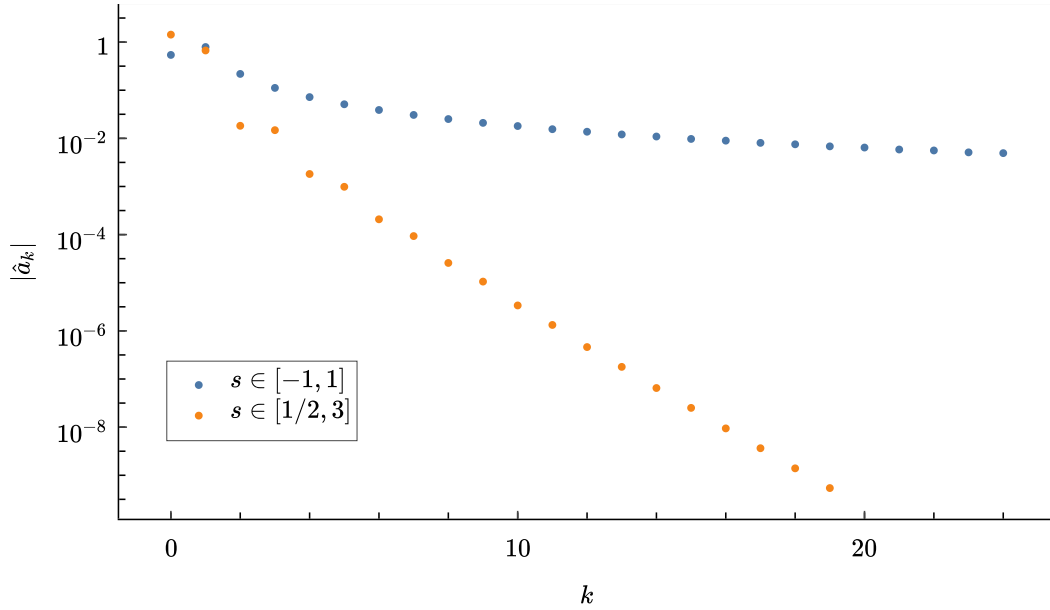


Figure 2: $|\hat{a}_k|$ versus k for $I_{\text{bub}}(s, m^2 = 1)$ over the intervals $s \in [-1, 1]$ (blue) and $s \in [1/2, 3]$ (orange) on a log scale. The flattening behavior of the first interval can be attributed to algebraic convergence, while the straight line behavior of the second interval can be attributed to geometric convergence.

where the x_k are the Chebyshev-Lobatto nodes and the double prime notation on the summation indicates that both the first and the last terms in the sum are to be halved. Given eq. (3.16), it follows that

$$\hat{a}_j = \frac{2}{w_j n} \sum_{k=0}^n {}''T_j(x_k) f(x_k), \quad (3.17)$$

where we make use of w_j defined as

$$w_0 = w_n = 2, \quad \text{and} \quad w_j = 1 \quad \text{otherwise.} \quad (3.18)$$

While one can take eq. (3.17) as a direct prescription for computing the interpolant coefficients, this can be further developed by considering eq. (3.17) more closely. First, we note that eq. (3.17) can be considered as a linear transformation acting on the vector of evaluations of $f(x)$ at the Chebyshev-Lobatto nodes. Specifically,

$$\hat{a}_j = \sum_{k=0}^n \mathcal{I}_{jk} f_k \quad (3.19)$$

where we have introduced the shorthand notation $f(x_k) = f_k$ and \mathcal{I}_{jk} is an $(n+1) \times (n+1)$ interpolation matrix. The entries of \mathcal{I}_{jk} are given by

$$\mathcal{I}_{jk} = \frac{2}{w_j w_k n} \cos\left(\frac{jk\pi}{n}\right), \quad (3.20)$$

where we have made use of eqs. (3.2) and (3.8) to re-express the evaluation of the Chebyshev polynomials directly in terms of the cosine function. Importantly, up to normalization factors, we see that the matrix \mathcal{I}_{jk} corresponds to the action of a so-called “discrete cosine transform” (DCT) of type 1. That is, the Chebyshev coefficients may be written as:

$$\hat{a}_j = \frac{2}{w_j n} \left[\frac{f_0}{2} + \sum_{k=1}^{n-1} \cos\left(\frac{jk\pi}{n}\right) f_k + (-1)^j \frac{f_n}{2} \right]. \quad (3.21)$$

In practice, the DCT can be implemented efficiently using so-called “fast cosine transform” approaches. One way to achieve this is to rephrase the DCT in terms of a discrete Fourier transform. To that end, we begin by defining the extended vector F_k of length $2n$ in the following manner:

$$F_k = \begin{cases} \tilde{f}_k, & 0 \leq k \leq n \\ \tilde{f}_{2n-k}, & n < k < 2n \end{cases} \quad (3.22)$$

where

$$\tilde{f}_k = \frac{1}{w_k} f_k. \quad (3.23)$$

The extended sequence is, by construction, even-symmetric, ensuring that only cosine modes contribute in the Fourier expansion. Consequently, we may calculate the Chebyshev interpolant coefficients in terms of a discrete Fourier transform as

$$\hat{a}_j = \frac{1}{w_j n} \sum_{k=0}^{2n-1} F_k e^{-2\pi i k j / 2n}, \quad (3.24)$$

which can naturally be evaluated efficiently using a fast Fourier transform (FFT) algorithm.

To close, let us consider the efficiency of each approach. The interpolation-matrix approach requires $\mathcal{O}(n^2)$ operations. In contrast, the DCT and FFT-based approaches require only $\mathcal{O}(n \log(n))$ operations. While for sufficiently large n the DCT/FFT-based approach is generally more efficient, for the moderate values of n encountered in Chebyshev approximation, the performance differences between these approaches are more strongly affected by the specifics of the implementation.

Evaluating a Chebyshev Series Once the Chebyshev series has been obtained, the next step is its evaluation at a given point $x \in [-1, 1]$. Direct evaluation of the series can become numerically unstable for large values of n due to round-off and cancellation errors. Clenshaw’s recurrence algorithm [56] is a computationally stable and efficient algorithm for evaluation, requiring $\mathcal{O}(n)$ operations. The algorithm can be applied to any family of functions satisfying a three-term recurrence relation. In the case of Chebyshev polynomials, they naturally satisfy a recursion relation given by

$$T_{n+1}(x) = 2xT_n(x) - T_{n-1}(x), \quad (3.25)$$

where the base case of the recursion is given by

$$T_0(x) = 1, \quad T_1(x) = x, \quad (3.26)$$

Algorithm 1: Clenshaw's Recurrence

Data: coefficients a_0, \dots, a_n , evaluation point x

Result: $y = \sum_{k=0}^n a_k T_k(x)$

$b_{n+1} \leftarrow 0;$

$b_{n+2} \leftarrow 0;$

for $k \leftarrow n$ **to** 0 *step* -1 **do**

$b_k \leftarrow a_k + 2x b_{k+1} - b_{k+2};$

end

$y \leftarrow b_0 - x b_1;$

return $y;$

which follows directly from eq. (3.2). One can thus make use of Clenshaw's algorithm which we describe in algorithm 1. For a comprehensive discussion of Clenshaw's algorithm, we refer the reader to standard texts in numerical analysis, such as refs. [57, 58].

Integrating a Chebyshev Series In the context of solving differential equations for Feynman integrals, our approach will be to construct a Chebyshev interpolant for the integrand in eq. (2.7), and to then integrate up this interpolant to find a Chebyshev approximation for the Feynman integral itself. As such, we need to be able to compute the Chebyshev series of the integral of some other Chebyshev series. Naturally, as Chebyshev polynomials form a basis of the vector space of all polynomials, the action of operators such as differentiation and integration of a Chebyshev polynomial may be represented as a linear combination of Chebyshev polynomials. Due to the connection of Chebyshev polynomials to trigonometric functions, i.e. eq. (3.2), it is not hard to see that integration of an arbitrary Chebyshev polynomial can be achieved in closed form. Specifically, it can be shown that

$$\int T_n(x) dx = \begin{cases} \frac{1}{2} \left[\frac{T_{n+1}(x)}{n+1} - \frac{T_{|n-1|}(x)}{n-1} \right] + C, & n \neq 1, \\ \frac{1}{4} T_2(x) + C, & n = 1, \end{cases} \quad (3.27)$$

for some constant of integration C . Similar results for differentiation can be found in ref. [52]. Thus we see that the indefinite integral of a Chebyshev series is itself a Chebyshev series of degree one higher than the original series. Using eq. (3.27), the coefficients of the antiderivative can be related to those of the original series as:

$$\int \sum_{k=0}^n a_k T_k(x) dx = C + \sum_{k=1}^{n+1} A_k T_k(x), \quad A_k = \begin{cases} a_0 - \frac{a_2}{2}, & k = 1 \\ \frac{a_{k-1} - a_{k+1}}{2k}, & k > 1, \end{cases} \quad (3.28)$$

where we implicitly take $a_{n+1} = a_{n+2} = 0$. As such, it is clear that integration of a (finite) Chebyshev series is a highly efficient operation that takes only $\mathcal{O}(n)$ operations. Although not directly relevant for our goal, we remark that an analogous result can be obtained for the derivative of a Chebyshev series [46], which can be useful for cross-check purposes.

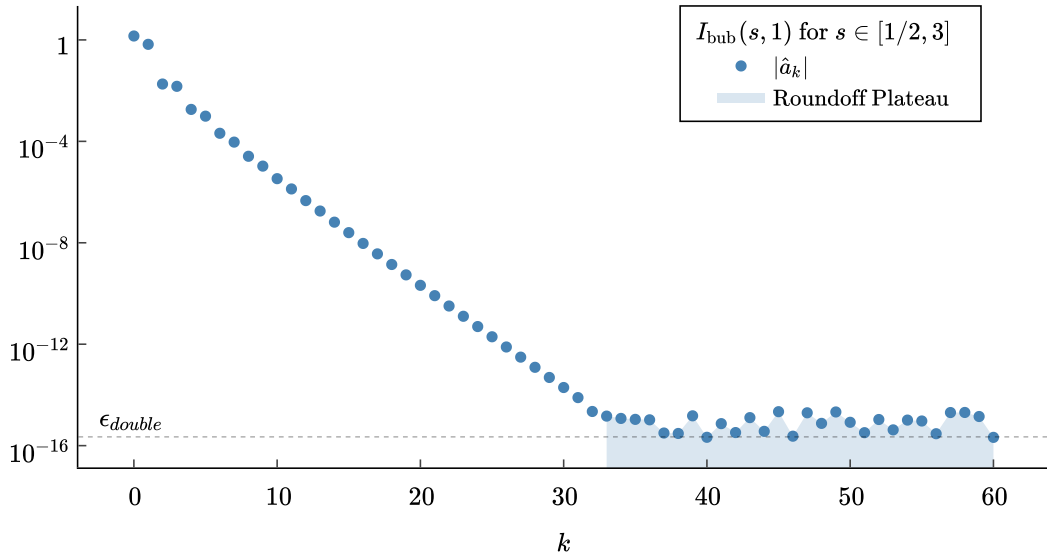


Figure 3: $|\hat{a}_k|$ versus k for $I_{\text{bub}}(s, m^2 = 1)$ over the interval $s \in [1/2, 3]$. The blue shaded region corresponds to the roundoff plateau for which roundoff errors associated with machine precision dominate the coefficient calculation. In this region, the coefficients oscillate around the roundoff error scale.

3.3 Numerical Convergence of Chebyshev Series

In order to practically build a Chebyshev interpolant for a univariate function, an important decision to make is to understand the order n of the Chebyshev approximation or, correspondingly, the number of nodes used for the collocation. As, in this work, we wish to apply Chebyshev collocation methods to analytic functions, it is natural to employ the error bound eq. (3.14) to guide this decision. In principle, this requires knowledge of the Bernstein radius of analyticity, ρ as well as the scale-setting constant M . While this could systematically be extracted from analytic knowledge of the function that we are interpolating, this requires case-by-case analysis. For this reason, we follow a numerical approach to understanding the convergence of a Chebyshev interpolant [47], as used in the `chebfun` project [45, 46].

Importantly, while the coefficients of the Chebyshev series of an analytic function exhibit geometric decay, in practical applications of Chebyshev series, one is confronted by numerical challenges in determining these coefficients. Indeed, as the coefficient magnitudes decrease, they inevitably reach the scale of the precision of the input data, beyond which the coefficients can no longer be computed accurately. At this stage, roundoff errors become the dominant source of error. This regime is known as the roundoff plateau. Within this region, the coefficients no longer decay exponentially but rather fluctuate randomly around the roundoff error scale. As the coefficients in the roundoff plateau are dominated by numerical noise, their computation offers little to no benefit. The task is thus to identify,

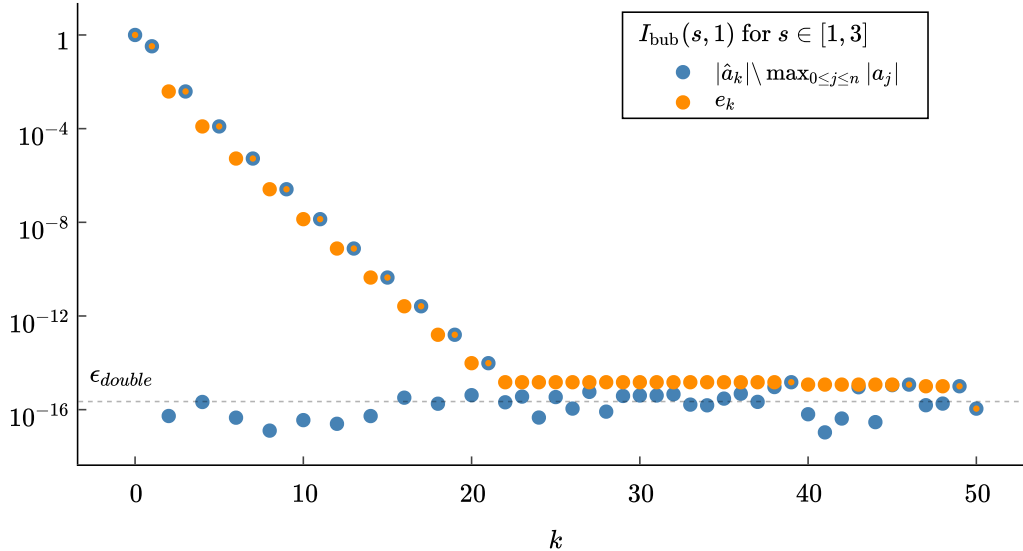


Figure 4: A depiction of the envelope of the sequence of (normalised) Chebyshev interpolant coefficients of $I_{\text{bub}}(s, m^2 = 1)$ on the interval $s \in [1, 3]$ for $n = 50$, alongside the normalised Chebyshev series. Bicoloured points denote points where the envelope and normalised coefficients are equal. The envelope acts as a filter, smoothing the oscillation of the expansion coefficients.

in an automatic and function-agnostic manner, the point beyond which the coefficients become corrupted by roundoff errors and to truncate the expansion accordingly.

Our approach is motivated by the observation that, when the absolute value of the expansion coefficients is plotted on a logarithmic scale, the roundoff plateau manifests itself as a region of relative flatness, with the coefficients oscillating about a median value (see fig. 3). If a straight line were to be fitted to the coefficients within this region, the resulting slope would be close to zero. By contrast, coefficients that remain relatively unaffected by roundoff errors are expected to display a strong negative slope corresponding to their exponential decay. Therefore, the task of identifying the roundoff plateau reduces to locating regions for which the local slope becomes sufficiently small. In what follows, we formalise this intuitive picture and provide a robust numerical implementation.

We begin by introducing the notion of an envelope of a sequence a_k , defined as [47]

$$e_j = \max_{j \leq k \leq n} |a_k|. \quad (3.29)$$

Provided that $e_0 \neq 0$, the sequence is normalised by e_0 , resulting in a non-negative, monotonically non-increasing sequence whose first element equals 1. The introduction of the envelope is motivated by two considerations. First, coefficients in a spectral expansion may exhibit oscillatory behaviour. For example, due to symmetry, all odd Chebyshev coefficients in the expansion of an even function vanish identically. The envelope filters

these oscillations, resulting in a smoother sequence while preserving the relevant underlying structure. Second, the envelope normalisation renders the algorithm scale-invariant, thereby mitigating the need to operate with coefficients whose magnitudes may potentially span several orders of magnitude.

In our applications, the important benefit of working with the envelope is that it allows for a practical way to identify the convergence rate of a Chebyshev series. When considering examples such as that in fig. 4, it is clear that the (logarithm) of the sequence can be approximated by a collection of straight lines. If one is able to robustly identify such a continuous model, this allows one to construct a simple notion of a derivative at any (even non-integer) point.⁵ To this end, we draw inspiration from recent applications of tropical geometry and Newton polygons/polytopes in the study of scattering amplitudes (see e.g. [59–65]). Specifically, to attach a continuous linear model to the logarithm of our envelope, we take its lower convex hull. As we work in two dimensions, this can be neatly expressed as

$$s(x) = \min_{\substack{i \neq j \\ i \leq x \leq j}} \left(\frac{j-x}{j-i} \log_{10}(e_i) + \frac{x-i}{j-i} \log_{10}(e_j) \right), \quad (3.30)$$

where the minimum is taken over i and j . We refer to $s(x)$ as a logarithmic “skeleton” of the envelope, that coarsely captures the structure of the non-increasing sequence. The skeleton is a piecewise linear function in log-space, whose graph is the lower facets of a convex polygon. The vertices of these facets can be efficiently computed from the envelope itself in $\mathcal{O}(n)$, for example, using the monotone chain algorithm. Importantly, as the skeleton is convex, its derivative is also a non-increasing function. To exemplify this, in fig. 5, we depict the envelope and logarithmic skeleton of the envelope for a Chebyshev approximation of the $I_{\text{bub}}(s, 1)$ on $s \in [1, 3]$. One can clearly see in this case that it is easy to identify from the skeleton where one reaches the roundoff plateau.

To practically define the location of the roundoff plateau we use a cutoff strategy, defining it as an $x_{\text{plateau}} \in [0, \tilde{n}]$ such that

$$s'(x_{\text{plateau}}) < \nabla_{\text{cutoff}}, \quad (3.31)$$

where $\tilde{n} < n$. We make use of \tilde{n} to ensure that the plateau is stable, and not only reached in the final coefficients, taking a value of $\tilde{n} = 0.85n$. In practice, we choose a gradient cutoff of $\nabla_{\text{cutoff}} = 0.02$. Beyond this, we only accept the plateau if the sum of the last five elements of the envelope sequence is less than 10^{-6} in order to explicitly ensure that the envelope has reached the asymptotic regime. If there is no x_{plateau} which satisfies these conditions, we conclude that the Chebyshev series has not yet converged. We will later use this “plateau test” to test for convergence in our adaptive algorithm. We note that ref. [47] uses a more sophisticated plateau detection criterion. While this would be interesting to investigate, we find that the simple cutoff approach is sufficient for phenomenological application and leave such investigations for further work.

⁵We note that this discussion represents a departure from the approach of ref. [47], principally motivated by the physicist’s desire to work with continuous objects.

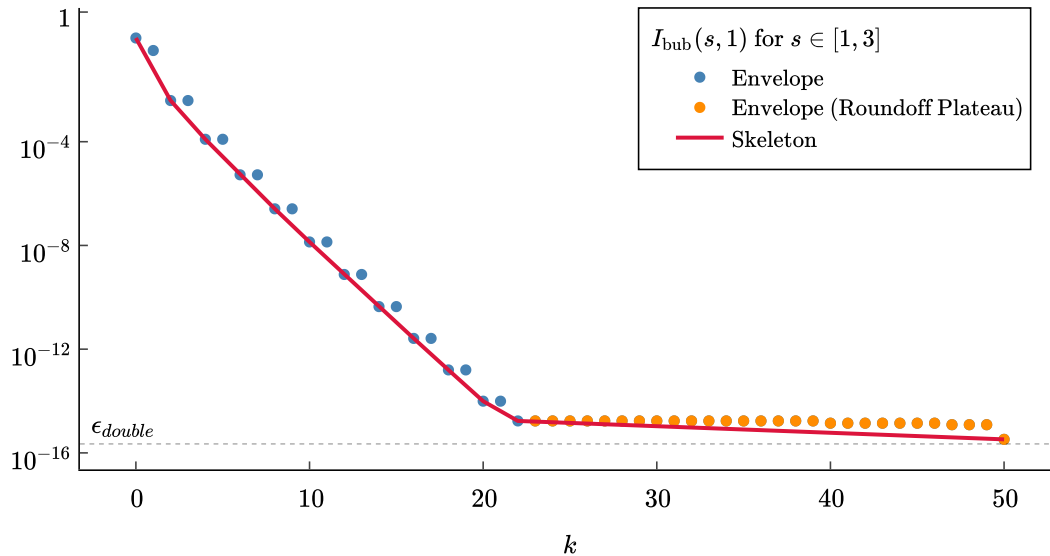


Figure 5: A depiction of the envelope of the sequence of Chebyshev interpolant coefficients of I_{bub} for $n = 50$, alongside its logarithmic skeleton. The logarithmic skeleton clearly provides a simple, nearly linear approximation to the envelope. The roundoff plateau (in orange) is clearly identified as a long flat stretch. Due to the simplicity of the input function, the roundoff plateau is controlled by the precision of machine floating point numbers.

Beyond using the plateau location to determine if a Chebyshev series has numerically converged, we can also use it to estimate the convergence rate. As discussed in section 3.1, for an analytic function, the gradient of the coefficient curve on a log-scale plot approximates $\log_{10}(\rho)$. Let us define $n_{\text{plateau}} = \text{floor}(x_{\text{plateau}})$ as the location in the sequence just before the plateau. We define an approximation to ρ as

$$\log_{10}(\rho_{\text{approx}}) = -\log_{10}(e_{n_{\text{plateau}}})/n_{\text{plateau}}. \quad (3.32)$$

This quantity, on the log-scale plot of the envelope gives some average derivative of the curve, thereby giving a coarse measure of the rate of convergence of the sequence. In our adaptive approach, ρ_{approx} will be useful to detect if a Chebyshev series on a particular range is converging at a sufficient rate and to act accordingly.

3.4 An Adaptive Chebyshev Approach for Feynman Integrals

Having introduced a sufficient collection of Chebyshev technology let us now discuss how we can use this to construct a robust algorithm to compute the integrals in eq. (2.7). Our approach is to construct a Chebyshev approximant for $\tilde{I}_i^{(n)}(\vec{s}[t])$ on the segment $t = [0, 1]$, in an iterative fashion. We assume the existence of a numerical black-box procedure for the evaluation of $\tilde{I}_i^{(n-1)}(\vec{s}[t])$. For $n = 1$, this is given by the weight 0 solutions to the integrals, which are rational numbers and easily computed analytically. For $n >$

1, we make use of the output of our procedure at a previous iteration. At fixed n , we construct a Chebyshev interpolant of the integrand in eq. (2.7). Given the discussion in section 3.2, we then perform the integration of the interpolant analytically, arriving at a Chebyshev approximation of the anti-derivative in eq. (2.7). Finally, we fix the constant of integration to match the boundary value $\tilde{I}_i^{(n)}(\vec{s}_0)$. We use Clenshaw’s algorithm to evaluate the Chebyshev approximant at \vec{s}_0 , finally arriving at a Chebyshev approximation for $\tilde{I}_i^{(n)}(\vec{s}[t])$ which can efficiently be evaluated anywhere along the path using Clenshaw’s algorithm.

The main ingredient in our procedure is thus to construct a Chebyshev interpolant of the integrand in eq. (2.7). Our approach is “adaptive”: we use the technology of section 3.3 to robustly stop sampling in the presence of roundoff error, and increase sampling density in the presence of nearby non-analyticities. For generality, we denote the function under approximation as $f(t)$ and the Chebyshev approximation range as $[t_0, t_1]$. Similar to commonly used series expansion methods (e.g. [21]), we achieve this by taking the original range and splitting it up into “segments”. We adaptively choose a segmentation based on the observed convergence properties of the Chebyshev approximation, leading to more dense sampling in regions of slower convergence.

A first consideration that must be discussed is the choice of map from a segment $[T_0, T_1]$ in t space to the range $[-1, 1]$ in Chebyshev space. Let us denote the Chebyshev variable by x . In practice, a map from t -space to x -space is simply an expression for x as a function of t . Analogously, this map can be inverted and we can consider t as a function of x . The simplest choice of map to Chebyshev space is an affine map. The affine map from $[-1, 1]$ to $[T_0, T_1]$, alongside its inverse are given by

$$t(x) = T_1 - (T_1 - T_0) \frac{1 - x}{2}, \quad (3.33)$$

$$x(t) = 1 - 2 \frac{T_1 - t}{T_1 - T_0}, \quad (3.34)$$

which is uniquely fixed by the fact that the map is linear, together with the requirement that $x(T_0) = -1$ and $x(T_1) = 1$.

While the affine map is simple, it can be useful to consider other choices of map to improve the convergence of Chebyshev approximation. Recalling the discussion in section 3.1, we note that the radius of the Bernstein ellipse can be limited by the presence of an algebraic branch point of $f(t)$ close to the segment $[T_0, T_1]$. Indeed, in practical applications to Feynman integrals, it frequently occurs that there is a square-root branch point at some $t_2 \notin [t_0, t_1]$ that can be associated with the vanishing of a Gram determinant. A natural solution to this is to choose a map to Chebyshev space such that, as a function of x , the argument of the square-root is locally a perfect square. Colloquially, we will say that this map “resolves” the square root branch point. A map from the segment $[T_0, T_1]$ to $[-1, 1]$

Algorithm 2: Adaptive Chebyshev Interpolation

Input: Function $f(t)$, range $[t_0, t_1]$

Set initial segment to full range, i.e. $[T_0, T_1] \leftarrow [t_0, t_1]$

1 Segment Initialise: Sample the segment on a mapped $n = 8$

Chebyshev-Lobatto grid and build the interpolant

2 Refine Segment:

if $\rho_{\text{approx}} < \rho_0$ **then go to 3**

if *Converged by plateau test* **then go to 4**

if $n < 128$ **then** Set $n \leftarrow 2n$, sample to build the interpolant, and **go to 2**

3 Bisect Segment: Set $T_1 \leftarrow T_0 + (T_1 - T_0)/2$ and **go to 1**

4 Next Segment: **if** $T_1 \neq t_1$ **then**

 Move to the remaining part of the range, setting $[T_0, T_1] \leftarrow [T_1, t_1]$

go to 1

end

that resolves a square root branch point at $t_2 \notin [t_0, t_1]$ is

$$t(x) = t_2 - (t_2 - T_0) \left(1 - \frac{1 - u(T_1)}{2} (x + 1) \right)^2, \quad (3.35)$$

$$x(t) = 2 \frac{1 - u(t)}{1 - u(T_1)} - 1, \quad (3.36)$$

where

$$u(t) = \sqrt{\frac{T_2 - t}{T_2 - T_0}}. \quad (3.37)$$

When using such a non-linear map to approximate $f(t)$ in a context where one desires to compute the anti-derivative, one is faced with the question of what to do with the Jacobian of the map. As it must eventually be included by the time of integration, when using a non-linear map, we choose to construct an approximation for $f(t)$ including the Jacobian factor. This choice has an important side effect. Specifically, if the square root singularity at $t = t_2$ is integrable, this behaviour is cancelled by the inclusion of the Jacobian factor. In practice, this allows our technology to interpolate functions with integrable singularities.

Let us now discuss our algorithm for constructing a Chebyshev approximation of a function $f(t)$ on a range $[t_0, t_1]$. We present the algorithm in algorithm 2. Starting with a tentative initial segment $[T_0, T_1] = [t_0, t_1]$, we sample on a small Chebyshev-Lobatto grid. Computing the associated Chebyshev coefficients, we then use these to decide how to proceed. We first check if the Chebyshev approximation seems to be converging. To this end, we compute ρ_{approx} and check if it is above some target value ρ_0 . If the convergence is not strong enough, we decide to bisect the segment. If the convergence behaviour is satisfactory, we next check to see if the approximation has already converged by the plateau test. If the approximation has not converged, we double the Chebyshev order and resample.

Importantly, as the Chebyshev-Lobatto grid for an interpolant of degree $2n$ contains the grid for degree n , one can recycle the known evaluations. We repeat this until either the approximation converges or we hit a cutoff of 128 samples. At this stage, we move on to process the remaining segment, or terminate.

The output of this approach is thus a collection of Chebyshev approximations of $\tilde{I}_i^{(n)}(\vec{s}[t])$, one for each segment, that can easily be evaluated at any point along the path. It thus allows us both to evaluate the integrals at the point of interest, \vec{s}_1 as well as provides input to the calculational procedure at weight $n + 1$.

We close with some technical comments on our implementation. Firstly, we note that algorithm 2 requires the specification of a “target” convergence rate ρ_0 . In our implementation, we choose $\log_{10}(\rho_0) = 0.2$. This is motivated by the ad-hoc desire to achieve an increase of precision of 1 digit for every 5 coefficients, therefore potentially reaching machine precision in around 80 evaluations. The sample cutoff of 128 in algorithm 2 is motivated as the smallest power of 2 beyond this expectation. In future work it would be interesting to understand the impact of the choice of ρ_0 on performance. Nevertheless, in practical applications we find this choice acceptable. Secondly, in practical implementation of our approach, sufficiently degenerate phase space points can be challenging. To ensure that the algorithm does not continue indefinitely due to such precision issues, we limit the number of segments to 25 and a minimal segment length of $10^{-7}(t_1 - t_0)$, and require that the final such segment always uses 128 samples. As a final comment, we note that an affine-mapped Chebyshev-Lobatto grid of order n covering $[T_0, T_1]$ and $[T_0, T_0 + (T_1 - T_0)/2]$ only share a small number of nodes. Thus, when the path is bisected, previous evaluations cannot be efficiently reused. This motivates our early and repeated detection of convergence behaviour.

4 Application to Pentagon Functions

A major aim of this work is to develop a general tool for solving canonical differential equations such as eq. (2.3) that is not tailored to a specific problem and is suitable for phenomenological applications. In this section, we stress test our approach by applying it to recompute various collections of two-loop five-point Feynman integrals. Specifically, we consider the numerical evaluation of pentagon functions for full-colour five-point massless processes and leading-colour five-point one-mass processes, which were first presented in a form suitable for phenomenological application in ref. [48] and ref. [49] respectively. In this section, we describe details of the application of our adaptive Chebyshev approximation approach, discuss its performance over phase-space, and provide a proof of concept `Mathematica` implementation in ancillary files [66].

4.1 Physical Phase Space for Five-Point Processes

In full generality, five-point Feynman integrals are functions of five momenta p_i , which satisfy total momentum conservation, i.e. $\sum_{i=1}^5 p_i^\mu = 0$, where we make use of the all incoming convention. The specifics of the on-shell conditions depends on the particular process under consideration, which we return to later. We are interested in evaluating

these collections of Feynman integrals at a point in the physical scattering channel

$$p_1, p_2 \rightarrow p_3, p_4, p_5. \quad (4.1)$$

We will achieve this by solving their differential equations by evolution over a path that lives entirely within physical phase space.

While physical phase space is most naturally described in momentum space, where scattering momenta that conserve total momentum are on-shell and real-valued and have the appropriate signs of their energy components, it is frequently the case that the differential equations are solved in the space of Mandelstam variables, $s_{ij} = (p_i + p_j)^2$ (and p_i^2 if external legs are massive). In terms of Mandelstam variables, the momentum-conservation and on-shellness constraints are easily solved, while the energy positivity constraints give rise to linear inequalities that the Mandelstam variables must satisfy. In contrast, the reality condition for the momenta translates into a non-trivial constraint on the Gram determinant associated to the five momenta,

$$G_5 = \det(\{p_i \cdot p_j\}_{i,j \in \{1, \dots, 4\}}). \quad (4.2)$$

In physical phase space, it is well known that the Gram determinant is negative [67]. That is,

$$G_5 < 0, \quad (4.3)$$

which follows from the physical metric signature.

In order to practically solve the differential equation, given an initial point \vec{s}_0 and a final point \vec{s}_1 , we must construct a path that lives entirely within physical phase-space. For simplicity, it is easiest to work with straight-line paths in Mandelstam space. That is, we consider a path of the form

$$\vec{s}[t] = \vec{s}_a(1 - t) + \vec{s}_b t. \quad (4.4)$$

However, it is well understood that the Gram negativity constraint, eq. (4.3), cuts out a non-convex, often not star-shaped region of Mandelstam space [48, 49]. In order to overcome this problem, we follow the approach of [49]. Specifically, we construct a path from \vec{s}_0 to \vec{s}_1 as a concatenation of straight-line paths, each of which lives entirely within the region of phase space under consideration. To do this, we first check if the straight line between \vec{s}_0 and \vec{s}_1 lives within physical phase space. If not, we repeatedly generate an intermediate physical point \vec{s}^* until the straight lines $\vec{s}_0 \rightarrow \vec{s}^*$ and $\vec{s}^* \rightarrow \vec{s}_1$ live within physical phase space. As expected from previous computations [48–50], we can always construct such a two-segment path, i.e. we can always find such a point \vec{s}^* .

The Gram determinant G_5 also plays an important role in the analytic structure of five-point Feynman integrals. Specifically, the collection of Feynman integrals that we study in this work have an algebraic branch point at $G_5 = 0$. As this is the boundary of phase space, and we choose to solve the differential equation along paths entirely within physical phase space, we will never cross this branch point. Nevertheless, in physical phase-space samples, points where G_5 is small can frequently be found, which has an important

weight	0	1	2	3	4
# massless functions	1	10	80	493	473
# one-mass functions	1	11	92	624	883

Table 1: Number of linearly independent functions at each weight that contribute to the two-loop full-colour massless squared amplitude and the leading-colour one-mass squared amplitude. The corresponding number of linearly independent master integrals is 1917 and 1383 for the massless and one-mass case, respectively.

impact on the convergence properties of our approach. We use this observation to guide the choice of mapping to Chebyshev space that was discussed in section 3.4. Specifically, we use the square-root branch-point resolving map of eqs. (3.35) and (3.36), choosing the point t_2 to be the location of the closest real zero of the Gram determinant G_5 . Naturally, for physical reasons, this is outside of the range $[0, 1]$. In practice, we see that this causes a noticeable decrease in the number of segments that the adaptive approach builds, providing an important speedup.

4.2 Numerical Study for Five-Point Massless and One-Mass Scattering

In this section, we study the behaviour of our numerical differential equation solution strategy over physical phase space. We make use of a proof-of-concept double-precision `Mathematica` implementation of our adaptive Chebyshev approach that we provide in ancillary files that are described in section 4.3. We consider two collections of two-loop five-point Feynman integrals. First, we consider the complete set of two-loop five-point massless Feynman integrals [68–73]. Second, we consider the complete set of two-loop five-point one-mass integrals relevant for the leading colour production of a W boson in association with two jets [74, 75]. We study both of these cases by using our `Mathematica` implementation to sample over phase space, and compare to higher precision evaluations provided by the C++ code, `PentagonFunctions++` [48, 49].

Let us begin by describing the invariant kinematics in the channel of eq. (4.1). The kinematics of the complete set of two-loop five-point massless Feynman integrals can be specified in terms of five independent Mandelstam variables,

$$\vec{s}^{\text{massless}} = \{s_{12}, s_{23}, s_{34}, s_{45}, s_{15}\}. \quad (4.5)$$

Here, energy positivity constrains the Mandelstam variables to satisfy the inequalities

$$s_{12}, s_{34}, s_{35}, s_{45} > 0, \quad s_{13}, s_{14}, s_{15}, s_{23}, s_{24}, s_{25} < 0. \quad (4.6)$$

For five-point one-mass scattering processes, we have that four of the external momenta are massless, while one of them is massive. We choose the massive momentum to be p_5 such that we have

$$p_i^2 = 0, \quad i \in \{1, 2, 3, 4\}, \quad p_5^2 = Q^2. \quad (4.7)$$

There are now six independent Mandelstam invariants given by

$$\vec{s}^{\text{5pt1m}} = \{s_{12}, s_{23}, s_{34}, s_{45}, s_{15}, p_5^2\}. \quad (4.8)$$

In this case, the linear constraints on the Mandelstam variables in eq. (4.8) are given by

$$s_{12}, s_{34} > 0, \quad s_{13}, s_{14}, s_{23}, s_{24} < 0, \quad s_{15}, s_{25} < Q^2, \quad s_{35}, s_{45} > Q^2. \quad (4.9)$$

To construct the system of differential equations for the pentagon functions we start from the differential equations of refs. [72] and [74]. We permute the system of differential equations and remove redundancies between the set of permuted Feynman integrals using FEYNHON [76]. We then use the approach of ref. [50] to construct a basis of pentagon functions $\tilde{I}_i^{(n)}$ up to weight 4. In a nutshell, the pentagon functions are chosen to be components of master integrals, relations between functions are obtained from linear algebra operations at symbol level and then lifted to function level using a single numerical evaluation.⁶ We report the number of linearly independent functions at each weight in table 1, as this controls the sizes of the differential equations that we must solve. In both cases, we used high-precision evaluations from the `PentagonFunctions++` library as boundary conditions [77].

To benchmark the performance of our differential equation solver, we test the implementation on a MacBook Pro equipped with an M5 Pro processor. We generate phase-space points in a flat manner using an internal `Mathematica` implementation of the RAMBO algorithm [78] such that the centre of mass energy s_{12} is normalised to 1. As an initial boundary point for the evolution, for the massless case, we select the phase-space point given by

$$\vec{s}_0^{\text{massless}} = \left\{ \frac{29}{10}, -\frac{202}{235}, \frac{679}{745}, \frac{1239}{1285}, -\frac{2544}{2705} \right\}, \quad (4.10)$$

while for the one-mass case, we use the boundary point⁷

$$\vec{s}_0^{\text{5pt1m}} = \left\{ 10, -\frac{7}{3}, \frac{9}{5}, \frac{13}{4}, -\frac{3}{2}, 1 \right\}. \quad (4.11)$$

We note that, unlike in ref. [48], $\vec{s}_0^{\text{massless}}$ is chosen such that it is not a star centre. As a star centre must lie on a spurious singularity surface, its use would introduce numerical complications when evaluating the integrands in eq. (2.7). Nevertheless, in practice, our chosen point is sufficiently well-behaved that only an insignificantly small number of phase-space points cannot be reached via a simple straight-line path. In contrast, for the one-mass case, we find that starting at \vec{s}_0^{5pt1m} requires us to construct a two-segment path around 8% of the time.

To validate the accuracy of our evaluations, we compare our double-precision implementation against evaluations obtained from the `PentagonFunctions++` library in quadruple precision. Note that our framework computes a large number of special functions simultaneously, thus we report the maximum relative error observed across the entire set

⁶We note that this approach differs slightly from that of refs. [48, 49], leading to a smaller number of functions. The numbers quoted in table 1 should thus not match with the ones given of refs. [48, 49]

⁷We note that this point is not in the kinematic region implemented in the `PentagonFunctions++` code, since the conventions there are that one should work in the channel $p_4, p_5 \rightarrow p_1, p_2, p_3$. It is a trivial relabeling to go from one channel to the other.

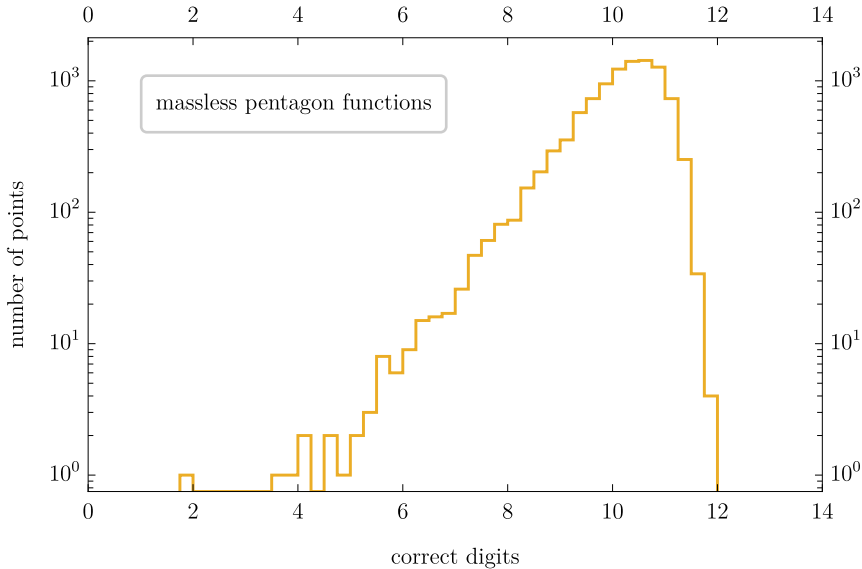


Figure 6: Precision study for five-point massless pentagon functions: distribution of correct digits, $-\log_{10}(E_r[\vec{s}])$, over 10^4 physical phase-space points as generated by RAMBO with s_{12} normalised to 1.

	Median (s)	Mean (s)	Max (s)
Massless	0.35	0.56	6.5
One-mass	1.2	1.45	10.7

Table 2: Timing characterization of proof-of-concept, double-precision, `Mathematica` implementation of adaptive Chebyshev differential equation solver to evaluate complete sets of pentagon functions. Variation over phase space can be attributed to the use of more segments with the adaptive strategy

of functions. Specifically, we define this error measure as

$$E_r(\vec{s}) = \max_{n, i} \left| 1 - \frac{\tilde{I}_i^{(n), \text{cheby}}(\vec{s})}{\tilde{I}_i^{(n), \text{p++}}(\vec{s})} \right|, \quad (4.12)$$

where the label “cheby” denotes that the function has been evaluated using the Chebyshev solver, and the label “p++” denotes that the function has been evaluated using the `PentagonFunctions++` code. In figs. 6 and 7 we plot the error as defined in eq. (4.12) across 10^4 phase-space points generated by RAMBO for the massless and one-mass configurations, respectively. We recall that all our evaluations are performed in double precision, and in our proof-of-principle implementation, we have not implemented any rescue system to correct the points where precision is lost. Despite this, we observe that precision is under excellent control, with catastrophic loss of precision in a vanishingly small number of points in the one-mass case. There are several strategies that can be explored to circumvent loss of precision within our algorithm, but we leave this for future work.

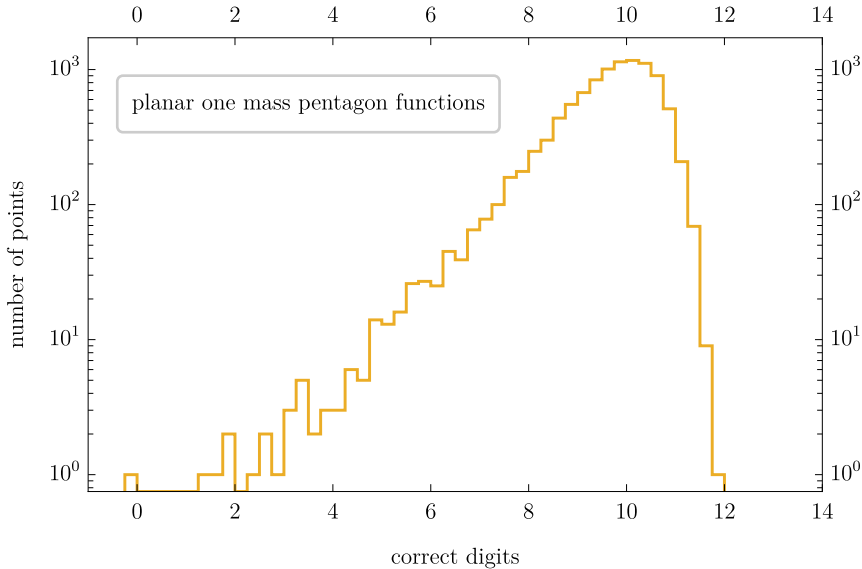


Figure 7: Precision study for five-point one-mass pentagon functions: distribution of correct digits, $-\log_{10}(E_r[\vec{s}])$, over 10^4 physical phase-space points as generated by RAMBO with s_{12} normalised to 1.

Finally, let us remark upon the performance of our implementation across phase space. We find that the evaluation is highly efficient, yielding timings that are competitive with the `PentagonFunctions++` code. We record characteristic timing evaluations in table 2. The difference in evaluation times can be attributed to a larger or smaller number of segments constructed by the algorithm. Notably, the fastest evaluations use only a single segment with $n = 16$. Naturally, we see that the runtimes for the one-mass case are higher than the massless case, which can be attributed to the larger size of the differential equation matrices.

4.3 Ancillary Files

We provide ancillary files that contain a proof-of-concept implementation of our adaptive Chebyshev differential-equation solver. The code has been used to produce the histograms in section 4.2. In order to facilitate understanding of the code, we provide example notebooks that can be used to evolve the two sets of pentagon functions from a boundary point to a second target point. Our ancillary files can be found at ref. [66] and are organised as follows:

- `/pfDefinition_massless`: Folder containing a script that defines the pentagon functions for all five-point massless integrals up to two loops. We give our conventions for the pure basis for the full space of integrals, and a map from those integrals to our definition of pentagon functions. The latter are the functions we evaluated with our adaptive Chebyshev differential-equation solver
- `/pfDefinition_1m`: The same as the folder above, now for the five-point one-mass

planar integrals up to two loops. We refer back to the comment in footnote 7: the conventions of ref. [74] and of the `PentagonFunctions++` are not directly compatible with the physical channel in eq. (4.1) and the conventions of eq. (4.7). This is, however, easily fixed by a trivial relabeling of the momenta.

- `source/chebyshev.m`: Proof-of-concept implementation of adaptive Chebyshev interpolation.
- `source/aux.wl`: Differential equation solution technology.
- `source/Grams.m`: Expressions for five-point Gram determinants.
- `DE/Alphabet_[5ptMassless,5ptOneMass].m`: Expressions for the letters W_k .
- `DE/DE_[5ptMassless,5ptOneMass].m`: Connection matrices $\tilde{M}_{ijk}^{(n)}$.
- `BC/*.m`: Benchmark boundary and target values.
- `[5ptMassless,5ptOneMass].wl`: Proof-of-concept notebooks demonstrating the evaluation of five-point massless and five-point one-mass pentagon functions with the Chebyshev approximation technology.

We note that the target point in the massless demonstration notebook was chosen to demonstrate one of the strengths of the approach, as it lives on a spurious singularity. Specifically, we choose the point

$$\vec{s}_1^{\text{massless}} = \{3, -1, 1, 1, -1\}. \quad (4.13)$$

Evaluation on $\vec{s}_1^{\text{massless}}$ would cause numerical issues if one were to construct a path that ends at $\vec{s}_1^{\text{massless}}$, as one of the Chebyshev nodes would lie on a spurious singularity. Instead, we construct the Chebyshev approximations on a path which contains the target point. Once the approximation is constructed, it can be used to evaluate the solution on any point along the path, and in particular at $\vec{s}_1^{\text{massless}}$, providing a simple way to sidestep the numerical issues.

Finally, we stress that the evaluation notebooks use straight-line paths and will give incorrect results if one modifies the final point such that the straight line leaves physical phase space. As noted previously, for the phase-space study in section 4.2, we implemented an algorithm to combine paths when a single straight path would leave phase space.

5 Summary and Outlook

In this work, we have explored the application of Chebyshev approximation techniques to the evaluation of Feynman integrals. The approach is motivated by its exponentially convergent behaviour for analytic functions, a characteristic that naturally complements the robust understanding of the analyticity properties of scattering amplitudes and Feynman integrals. We have introduced an adaptive Chebyshev approximation framework tailored for solving canonical differential equations for linearly-independent sets of special functions.

This method dynamically detects the convergence of the approximation by employing the plateau test of ref. [47], avoiding oversampling in the presence of round-off errors or non-analyticities near the region of approximation. Using this approach, we have been able to demonstrate excellent control over precision across physical phase space. Furthermore, we have shown that it is straightforward to construct an implementation that relies purely on standard machine precision arithmetic. As a practical proof of concept, we provided a **Mathematica** implementation of two-loop five-point massless pentagon functions and one-mass planar pentagon functions that exhibits run times which are competitive with current implementations in compiled languages [48, 49]. Crucially, the approach is strongly flexible: once a canonical differential equation is available, it can be easily and rapidly integrated within the Chebyshev framework.

Looking forward, we see several directions to explore for future research. A natural next step is the direct application of this framework to more demanding kinematics, such as the collection of recently computed two-loop six-point Feynman integrals [79–82]. Moreover, in order to be able to apply the technique to phenomenological studies, it will be important to develop a public implementation optimised for cluster-scale applications, and if possible in a compiled language that would further improve the already excellent timings of our approach. Furthermore, it would be highly interesting to extend this approach to the treatment of five-point integrals with more external or even internal masses, that can involve many roots or even elliptic sectors [83–87]. Finally, it would be interesting to consider a systematic study of the computation of Feynman integrals in singular regions where massless particles become soft or collinear, for application to real/virtual contributions to physical cross sections.

Note added: While this manuscript was in the final stages of preparation, the preprint [88] appeared, which also provides a public Chebyshev approximation method for Feynman integrals.

Acknowledgements

We would like to thank S. Devoto, M. Kraus, X. Liu and P.F. Monni for helpful discussions and collaboration on related projects. The work of A. Guerreiro is supported by Fundação para a Ciência e a Tecnologia (FCT) under the contract 2025.03095.BD.

References

- [1] G. Heinrich, *Collider physics at the precision frontier*, *Physics Reports* **922** (Aug., 2021) .
- [2] A. Huss, J. Huston, S. Jones, M. Pellen and R. Röntsch, *Les houches 2023 – physics at tev colliders: Report on the standard model precision wishlist*, *SciPost Physics Community Reports* (Mar., 2026) .
- [3] R. Aliberti, T. Aoyama, E. Balzani, A. Bashir, G. Benton, J. Bijnens et al., *The anomalous magnetic moment of the muon in the standard model: an update*, *Physics Reports* **1143** (Nov., 2025) 1–158.

- [4] K. G. Chetyrkin and F. V. Tkachov, *Integration by parts: The algorithm to calculate β -functions in 4 loops*, *Nucl. Phys. B* **192** (1981) 159–204.
- [5] S. Laporta, *High-precision calculation of multiloop Feynman integrals by difference equations*, *Int. J. Mod. Phys. A* **15** (2000) 5087–5159, [[hep-ph/0102033](#)].
- [6] F. Lange, J. Usovitsch and Z. Wu, *Kira 3: integral reduction with efficient seeding and optimized equation selection*, [2505.20197](#).
- [7] A. V. Smirnov and M. Zeng, *FIRE 7: Automatic Reduction with Modular Approach*, [2510.07150](#).
- [8] A. von Manteuffel and C. Studerus, *Reduze 2 - Distributed Feynman Integral Reduction*, [1201.4330](#).
- [9] X. Guan, X. Liu, Y.-Q. Ma and W.-H. Wu, *Blade: A package for block-triangular form improved Feynman integrals decomposition*, *Comput. Phys. Commun.* **310** (2025) 109538, [[2405.14621](#)].
- [10] R. N. Lee, *LiteRed 1.4: a powerful tool for reduction of multiloop integrals*, *J. Phys. Conf. Ser.* **523** (2014) 012059, [[1310.1145](#)].
- [11] Z. Wu, J. Böhm, R. Ma, J. Usovitsch, Y. Xu and Y. Zhang, *Performing integration-by-parts reductions using NeatIBP 1.1 + Kira*, *Comput. Phys. Commun.* **316** (2025) 109798, [[2502.20778](#)].
- [12] V. A. Smirnov, *Feynman integral calculus*. Springer, Berlin, Heidelberg, 2006.
- [13] S. Weinzierl, *Feynman Integrals. A Comprehensive Treatment for Students and Researchers*. UNITEXT for Physics. Springer, 2022. 10.1007/978-3-030-99558-4.
- [14] A. V. Kotikov, *Differential equations method: New technique for massive Feynman diagrams calculation*, *Phys. Lett. B* **254** (1991) 158–164.
- [15] A. V. Kotikov, *Differential equation method: The Calculation of N point Feynman diagrams*, *Phys. Lett. B* **267** (1991) 123–127.
- [16] Z. Bern, L. J. Dixon and D. A. Kosower, *Dimensionally regulated pentagon integrals*, *Nucl. Phys. B* **412** (1994) 751–816, [[hep-ph/9306240](#)].
- [17] E. Remiddi, *Differential equations for feynman graph amplitudes*, *Il Nuovo Cimento A* **110** (Dec., 1997) 1435–1452.
- [18] T. Gehrmann and E. Remiddi, *Differential equations for two-loop four-point functions*, *Nuclear Physics B* **580** (2000) 485–518.
- [19] J. M. Henn, *Multiloop integrals in dimensional regularization made simple*, *Phys. Rev. Lett.* **110** (2013) 251601, [[1304.1806](#)].
- [20] R. N. Lee, A. V. Smirnov and V. A. Smirnov, *Solving differential equations for feynman integrals by expansions near singular points*, *Journal of High Energy Physics* **2018** (Mar., 2018) .
- [21] F. Moriello, *Generalised power series expansions for the elliptic planar families of Higgs + jet production at two loops*, *JHEP* **01** (2020) 150, [[1907.13234](#)].
- [22] M. Hidding, *DiffExp, a Mathematica package for computing Feynman integrals in terms of one-dimensional series expansions*, *Comput. Phys. Commun.* **269** (2021) 108125, [[2006.05510](#)].

- [23] T. Armadillo, R. Bonciani, S. Devoto, N. Rana and A. Vicini, *Evaluation of Feynman integrals with arbitrary complex masses via series expansions*, *Comput. Phys. Commun.* **282** (2023) 108545, [2205.03345].
- [24] X. Liu, Y.-Q. Ma and C.-Y. Wang, *A systematic and efficient method to compute multi-loop master integrals*, *Physics Letters B* **779** (Apr., 2018) 353–357.
- [25] X. Liu and Y.-Q. Ma, *Multiloop corrections for collider processes using auxiliary mass flow*, *Physical Review D* **105** (Mar., 2022) .
- [26] X. Liu and Y.-Q. Ma, *AMFlow: A Mathematica package for Feynman integrals computation via auxiliary mass flow*, *Comput. Phys. Commun.* **283** (2023) 108565, [2201.11669].
- [27] R. M. Prisco, J. Ronca and F. Tramontano, *LINE: Loop Integrals Numerical Evaluation*, *JHEP* **07** (2025) 219, [2501.01943].
- [28] S. Badger, M. Becchetti, C. Brancaccio, M. Czakon, H. B. Hartanto, R. Poncelet et al., *Double virtual QCD corrections to $t\bar{t}$ +jet production at the LHC*, *JHEP* **05** (2026) 044, [2511.11424].
- [29] S. Badger, C. Brancaccio, M. Becchetti, M. Czakon, H. B. Hartanto, R. Poncelet et al., *Higher-order QCD corrections to top-quark pair production in association with a jet*, 2511.11431.
- [30] P. Petit Rosàs and W. J. Torres Bobadilla, *Fast evaluation of Feynman integrals for Monte Carlo generators*, *JHEP* **09** (2025) 210, [2507.12548].
- [31] M. Czakon and L. Tancredi, *Solution of Canonical Differential Equations for Integrals on Arbitrary Geometries*, 2606.30354.
- [32] G. Baur and C. Duhr, *IterInt: Evaluating iterated integrals via differential equations*, 2606.02744.
- [33] Y. Liu, A. Matijašić, T. Peraro, Y. Xu, Z. Yang and Y. Zhang, *Two-loop Six-point Planar Massless Feynman Integrals to Higher ϵ Orders*, 2603.16831.
- [34] C. Canuto, M. Y. Hussaini, A. Quarteroni and T. A. Zang, *Spectral Methods in Fluid Dynamics*. 1988. 10.1007/978-3-642-84108-8.
- [35] C. Canuto, M. Hussaini, A. Quarteroni and T. Zang, *Spectral Methods: Fundamentals in Single Domains*. Scientific Computation. Springer Berlin Heidelberg, 2007.
- [36] C. Temperton, *On scalar and vector transform methods for global spectral models*, *Monthly Weather Review* **119** (1991) 1303 – 1307.
- [37] P. Grandclément and J. Novak, *Spectral methods for numerical relativity*, *Living Reviews in Relativity* **12** (Jan., 2009) .
- [38] M. Helmer and F. Tellander, *Geometric singularities of Feynman integrals*, *Phys. Rev. D* **112** (2025) 065019, [2506.05042].
- [39] S. Mizera and S. Telen, *Landau discriminants*, *JHEP* **08** (2022) 200, [2109.08036].
- [40] C. Fevola, S. Mizera and S. Telen, *Landau Singularities Revisited: Computational Algebraic Geometry for Feynman Integrals*, *Phys. Rev. Lett.* **132** (2024) 101601, [2311.14669].
- [41] C. Fevola, S. Mizera and S. Telen, *Principal Landau determinants*, *Comput. Phys. Commun.* **303** (2024) 109278, [2311.16219].

- [42] M. Correia, M. Giroux and S. Mizera, *SOFIA: Singularities of Feynman integrals automatized*, *Comput. Phys. Commun.* **320** (2026) 109970, [[2503.16601](#)].
- [43] M. Helmer, G. Papathanasiou and F. Tellander, *Landau Singularities from Whitney Stratifications*, [2402.14787](#).
- [44] C. Dlapa, M. Helmer, G. Papathanasiou and F. Tellander, *Symbol alphabets from the Landau singular locus*, *JHEP* **10** (2023) 161, [[2304.02629](#)].
- [45] T. A. Driscoll, N. Hale and L. N. Trefethen, eds., *Chebfun Guide*. Pafnuty Publications, Oxford, 2014.
- [46] Z. Battles and L. N. Trefethen, *An extension of matlab to continuous functions and operators*, *SIAM Journal on Scientific Computing* **25** (2004) 1743–1770, [<https://doi.org/10.1137/S1064827503430126>].
- [47] J. L. Aurentz and L. N. Trefethen, *Chopping a Chebyshev Series*, *arXiv e-prints* (Dec., 2015) [arXiv:1512.01803](#), [[1512.01803](#)].
- [48] D. Chicherin and V. Sotnikov, *Pentagon Functions for Scattering of Five Massless Particles*, *JHEP* **20** (2020) 167, [[2009.07803](#)].
- [49] D. Chicherin, V. Sotnikov and S. Zoia, *Pentagon functions for one-mass planar scattering amplitudes*, *JHEP* **01** (2022) 096, [[2110.10111](#)].
- [50] S. Abreu, D. Chicherin, H. Ita, B. Page, V. Sotnikov, W. Tschernow et al., *All Two-Loop Feynman Integrals for Five-Point One-Mass Scattering*, *Phys. Rev. Lett.* **132** (2024) 141601, [[2306.15431](#)].
- [51] L. N. Trefethen, *Approximation Theory and Approximation Practice, Extended Edition*. Society for Industrial and Applied Mathematics, Philadelphia, PA, 2019. [10.1137/1.9781611975949](#).
- [52] J. Mason and D. C. Handscomb, *Chebyshev Polynomials*. Chapman and Hall/CRC, 2002. [10.1201/9781420036114](#).
- [53] S. Bernstein, *Sur l'ordre de la meilleure approximation des fonctions continues par des polynômes de degré donné*, *Mémoires de l'Académie royale de Belgique* **4** (1912) 1–104.
- [54] S. Bernstein, *Sur la meilleure approximation de $|x|$ par des polynômes de degrés donnés*, *Acta Mathematica* **37** (1914) 1–57.
- [55] J. P. Boyd, *Chebyshev and Fourier Spectral Methods*. Courier Corporation, 2013.
- [56] C. W. Clenshaw, *A note on the summation of chebyshev series*, *Mathematics of Computation* **9** (1955) 118–120.
- [57] E. Cheney and D. Kincaid, *Numerical Mathematics and Computing*. Cengage Learning, 2012.
- [58] W. H. Press, ed., *Numerical Recipes: The Art of Scientific Computing*. Cambridge University Press, 3 ed., 2007.
- [59] G. Salvatori, *The Tropical Geometry of Subtraction Schemes*, [2406.14606](#).
- [60] M. Giroux, S. Mizera and G. Salvatori, *SubTropica*, [2604.20954](#).
- [61] M. Borinsky, *Tropical Monte Carlo quadrature for Feynman integrals*, *Ann. Inst. H. Poincaré D Comb. Phys. Interact.* **10** (2023) 635–685, [[2008.12310](#)].
- [62] M. Borinsky, H. J. Munch and F. Tellander, *Tropical Feynman integration in the Minkowski regime*, *Comput. Phys. Commun.* **292** (2023) 108874, [[2302.08955](#)].

- [63] G. Heinrich, S. Jahn, S. P. Jones, M. Kerner, F. Langer, V. Magerya et al., *Expansion by regions with pySecDec*, *Comput. Phys. Commun.* **273** (2022) 108267, [[2108.10807](#)].
- [64] A. Pak and A. Smirnov, *Geometric approach to asymptotic expansion of Feynman integrals*, *Eur. Phys. J. C* **71** (2011) 1626, [[1011.4863](#)].
- [65] N. Arkani-Hamed, A. Hillman and S. Mizera, *Feynman polytopes and the tropical geometry of UV and IR divergences*, *Phys. Rev. D* **105** (2022) 125013, [[2202.12296](#)].
- [66] S. Abreu, A. Guerreiro and B. Page, *Ancillary files for “Chebyshev Approximations of Feynman Integrals for Collider Physics”*, 2026. 10.5281/zenodo.21134108.
- [67] N. Byers and C. N. Yang, *Physical Regions in Invariant Variables for n Particles and the Phase-Space Volume Element*, *Rev. Mod. Phys.* **36** (1964) 595–609.
- [68] T. Gehrmann, J. M. Henn and N. A. Lo Presti, *Analytic form of the two-loop planar five-gluon all-plus-helicity amplitude in QCD*, *Phys. Rev. Lett.* **116** (2016) 062001, [[1511.05409](#)].
- [69] T. Gehrmann, J. M. Henn and N. A. Lo Presti, *Pentagon functions for massless planar scattering amplitudes*, *JHEP* **10** (2018) 103, [[1807.09812](#)].
- [70] S. Abreu, B. Page and M. Zeng, *Differential equations from unitarity cuts: nonplanar hexa-box integrals*, *JHEP* **01** (2019) 006, [[1807.11522](#)].
- [71] D. Chicherin, T. Gehrmann, J. M. Henn, N. A. Lo Presti, V. Mitev and P. Wasser, *Analytic result for the nonplanar hexa-box integrals*, *JHEP* **03** (2019) 042, [[1809.06240](#)].
- [72] S. Abreu, L. J. Dixon, E. Herrmann, B. Page and M. Zeng, *The two-loop five-point amplitude in $\mathcal{N} = 4$ super-Yang-Mills theory*, *Phys. Rev. Lett.* **122** (2019) 121603, [[1812.08941](#)].
- [73] D. Chicherin, T. Gehrmann, J. M. Henn, P. Wasser, Y. Zhang and S. Zoia, *All Master Integrals for Three-Jet Production at Next-to-Next-to-Leading Order*, *Phys. Rev. Lett.* **123** (2019) 041603, [[1812.11160](#)].
- [74] S. Abreu, H. Ita, F. Moriello, B. Page, W. Tschernow and M. Zeng, *Two-Loop Integrals for Planar Five-Point One-Mass Processes*, *JHEP* **11** (2020) 117, [[2005.04195](#)].
- [75] D. D. Canko, C. G. Papadopoulos and N. Syrrakos, *Analytic representation of all planar two-loop five-point Master Integrals with one off-shell leg*, *JHEP* **01** (2021) 199, [[2009.13917](#)].
- [76] V. Maheria, *Semi- and Fully-Inclusive Phase-Space Integrals at Four Loops*. PhD thesis, Hamburg U., 2022.
- [77] <https://gitlab.com/pentagon-functions>.
- [78] R. Kleiss, W. J. Stirling and S. D. Ellis, *A New Monte Carlo Treatment of Multiparticle Phase Space at High-energies*, *Comput. Phys. Commun.* **40** (1986) 359.
- [79] J. Henn, T. Peraro, Y. Xu and Y. Zhang, *A first look at the function space for planar two-loop six-particle Feynman integrals*, *JHEP* **03** (2022) 056, [[2112.10605](#)].
- [80] S. Abreu, P. F. Monni, B. Page and J. Usovitsch, *Planar six-point Feynman integrals for four-dimensional gauge theories*, *JHEP* **06** (2025) 112, [[2412.19884](#)].
- [81] J. M. Henn, A. Matijašić, J. Miczajka, T. Peraro, Y. Xu and Y. Zhang, *A computation of two-loop six-point Feynman integrals in dimensional regularization*, *JHEP* **08** (2024) 027, [[2403.19742](#)].

- [82] J. Henn, A. Matijašić, J. Miczajka, T. Peraro, Y. Xu and Y. Zhang, *Complete Function Space for Planar Two-Loop Six-Particle Scattering Amplitudes*, *Phys. Rev. Lett.* **135** (2025) 031601, [[2501.01847](#)].
- [83] F. Febres Cordero, G. Figueiredo, M. Kraus, B. Page and L. Reina, *Two-loop master integrals for leading-color $pp \rightarrow t\bar{t}H$ amplitudes with a light-quark loop*, *JHEP* **07** (2024) 084, [[2312.08131](#)].
- [84] S. Abreu, D. Chicherin, V. Sotnikov and S. Zoia, *Two-loop five-point two-mass planar integrals and double Lagrangian insertions in a Wilson loop*, *JHEP* **10** (2024) 167, [[2408.05201](#)].
- [85] S. Badger, M. Becchetti, N. Giraudo and S. Zoia, *Two-loop integrals for $t\bar{t}$ +jet production at hadron colliders in the leading colour approximation*, *JHEP* **07** (2024) 073, [[2404.12325](#)].
- [86] M. Becchetti, C. Dlapa and S. Zoia, *Canonical differential equations for the elliptic two-loop five-point integral family relevant to $t\bar{t}^-$ +jet production at leading color*, *Phys. Rev. D* **112** (2025) L031501, [[2503.03603](#)].
- [87] M. Becchetti, D. Canko, V. Chestnov, T. Peraro, M. Pozzoli and S. Zoia, *Two-loop Feynman integrals for leading colour $t\bar{t}W$ production at hadron colliders*, *JHEP* **07** (2025) 001, [[2504.13011](#)].
- [88] Y. Liu and Y. Zhang, *CHESS: CHEbyshev pSeudo-Spectral transport for Feynman integral differential equations*, [2606.26691](#).